Seismicity at Lusi and the adjacent volcanic complex, Java, Indonesia

Anne Obermann[1], Karyono Karyono[2,3,4], Tobias Diehl[1], Matteo Lupi[5], Adriano Mazzini[2]

[1]Swiss Seismological Service, ETH Zurich, Switzerland
[2]CEED, University of Oslo, Norway
[3]Padjadjaran University (UNPAD), Bandung, Indonesia
[4]Agency for Meteorology, Climatology and Geophysics (BMKG), Jakarta, Indonesia
[5]Department of Earth Sciences, University of Geneva, Switzerland

Abstract

We study the local seismicity in East Java around the Arjuno-Welirang volcanic complex that is connected via the Watukosek Fault System, to the spectacular Lusi eruption site. Lusi is a sediment-hosted hydrothermal system which has been erupting since 2006. It is fed by both mantellic and hydrothermal fluids, rising and mixing with the thermogenic gases and other fluids from shallower sedimentary formations. During a period of 24 months, we observe 156 micro-seismic earthquakes with local magnitudes ranging from M_L0.5 to M_L1.9, within our network. The events predominantly nucleate at depths of 8-13 km below the Arjuno-Welirang volcanic complex. Despite the geological evidence of active tectonic deformation and faulting observed at the surface, practically no seismicity is observed in the sedimentary basin hosting Lusi. Although we cannot entirely rule out artifacts due to an increased detection threshold in the sedimentary basin, the deficit in significant seismicity suggests aseismic deformation beneath Lusi due to the large amount of fluids that may lubricate the fault system. An analysis of focal mechanisms of nine selected events around the Arjuno-Welirang volcanic complex indicates predominantly strike-slip faulting activity in the region SW of Lusi. This type of activity is consistent with observable features such as fault escarpment, river deviation and railroad deformation; suggesting that the Watukosek fault system extends from the volcanic complex towards the NE of Java. Our results point out that the tectonic deformation of the region is characterized by a segmented fault system being part of a broader damage zone, rather than localized along a distinct fault plane.

1. Introduction

Numerous boiling mud eruptions appeared on May 29th 2006 in the Sidoarjo district, East Java. The eruption sites formed a 1.2 km long lineament with NE-SW direction (Cyranoski,

2007; Mazzini et al., 2007). At the same time, numerous fractures with the same orientation were observed at different localities in the region (Istadi et al., 2009; Mazzini et al., 2009). The predominant orientation of these fractures is sub-parallel to the Watukosek fault system (WFS, Mazzini et al. 2007). This strike slip system extends towards the NE from the Arjuno-Welirang (AW) volcanic complex, outcrops at the Watukosek escarpment, on the flanks of the Penanggungan (PG) volcano, bends the course of the Porong River, intersects Lusi and continues towards the NE Java basin hosting other mud volcanoes (Istadi et al, 2009, 2012, Mazzini et al, 2009, Roberts et al. 2011) (Fig. 1).

One of the craters was particularly active and covered a vast area of 1.5 km^2 in hot mud breccia within weeks after its appearance (van Noorden 2006). This prominent active crater was named Lusi (LUmpur-SIdoarjo) (Fig.1). More than 10 years later, Lusi is still active and erupting vigorously (i.e. about 70-80.000 m^3/day, Dec. 2016). Today a 10 m tall embankment surrounds a region of 7 km2 and contains the mud flooding. Lusi is characterized by a geysering behavior with periods of enhanced activity that coincides with tremors (Karyono et al., 2016) and vigorous expulsion of mud breccia and fluids (Mazzini et al., 2007; Mazzini et al., 2012; Vanderkluysen et al., 2014). Geochemical analyses of the erupted fluids revealed that Lusi is connected with the neighboring AW volcanic complex (Mazzini et al. 2012, Mazzini et al 2017, Inguaggiato et al 2017, Sciarra et al 2017). Its closest volcanic cone, PG, is located about 10 km SW of Lusi (Fig. 1).

From January 2015 to December 2016, we installed a network of 31 seismic stations covering Lusi, the WFS and the AW volcanic complex (Fig. 1). The goal of the present study is the analysis of the ongoing seismicity in the region and the imaging of potential connections between the back-arc basin, hosting Lusi, and the volcanic arc. Such a connection has been observed in previous studies as new fractures, embankment walls breaching, antithetic fractures, seeping pools distributions and abrupt rising in water temperatures at Lusi after seismic activity or volcanic eruptions in the region (Mazzini et al. 2007, 2009, 2012, Collignon et al. 2016).

2. Methods

2.1 Local seismic network

The temporary seismic network consisted of 10 broadband (Guralp CMG3T sensors in combination with EarthData EDR-210 Loggers (EDL)) and 21 short-period (16 1s LE-3Dlite Lennartz with Nanometrics digitizer and 5 Mark L-4-3D sensors with EDL) seismic stations

covering Lusi and the adjacent AW volcanic complex (Fig.1). For this study, we consider P-wave arrival times from local earthquakes recorded during the 24 months of deployment.

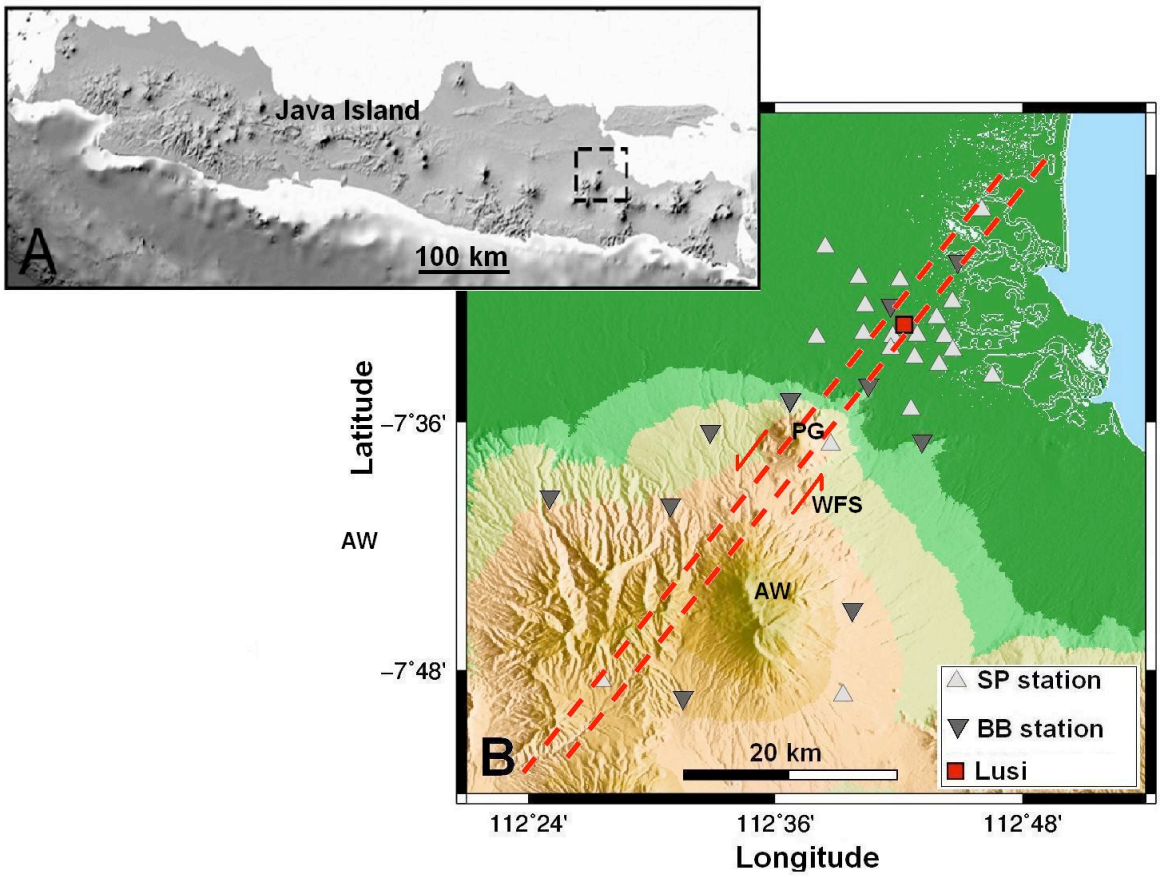

Figure 1: *Overview of the investigated area. A) Map of Java, Indonesia. The black square indicates the area of interest shown in B). B) Seismic network covering the Arjuno-Welirang volcanic complex (AW),* Penanggungan volcano (PG) *and the area around the Lusi eruption site (red square) in Eastern Java. The monitoring network consists of 10 broadband (dark-grey inverted triangles) and 21 short period stations (grey triangles). Red dashed lines indicate the inferred location of the Watukosek Fault Zone (WFS).*

We compute the station noise levels with the software PQLX (McNamara and Boaz 2006), which computes probability density functions (PDF) of the power spectral density (PSD) of the ground motion observed at a station (Fig. 2). From the PDF of the whole installation period of a station, we derive the statistical mode, 5 and 95 percentiles representing the most probable noise level at a station and its variation in the frequency range of 0.01 Hz to 100 Hz.

The sedimentary basin surrounding Lusi (Fig. 1B) is a densely populated area. We encounter moderate to poor signal-to-noise conditions, especially on the short-period stations in this area (Fig. 2, black). The short-period stations can be clearly distinguished from the broadband

stations in Fig. 2 due to the linearly increasing noise level below their cut-off frequency of 0.1 Hz. The stations around the volcanic complex were installed on bedrock and have better noise conditions (Fig. 2, red). We observe a peak noise band around 2-3 Hz that is particularly dominant on the basin stations and disappears on the stations further into the AW volcanic complex. This noise peak is likely due to resonance effects and cultural noise in the densely populated basin.

We compare the station noise levels to synthetic S-wave source spectra for earthquakes between magnitudes M_L-1.5 to M_L2.5. The source spectra are calculated assuming a Brune source (Brune, 1970, 1971) with a stress drop of 2.1 MP at a hypocentral distance of 2 km. For easier comparison we convert PSD-amplitudes to octave band-passed velocity (e.g., Bormann, 1998; Clinton and Heaton, 2002). The comparison shown in Fig. 2 suggests that the ambient noise level at sedimentary sites is higher than the expected signal amplitude of synthetic earthquakes with magnitudes smaller or equal to M_L0.5 in the frequency band of interest for this study (1–30 Hz). However, the synthetic spectra might deviate from the real data recorded in the basin due to expected differences in the attenuation. The threshold above which all earthquakes in the area are recorded (magnitude of completeness) might therefore be higher and we cannot claim to achieve completeness of the catalog in this area.

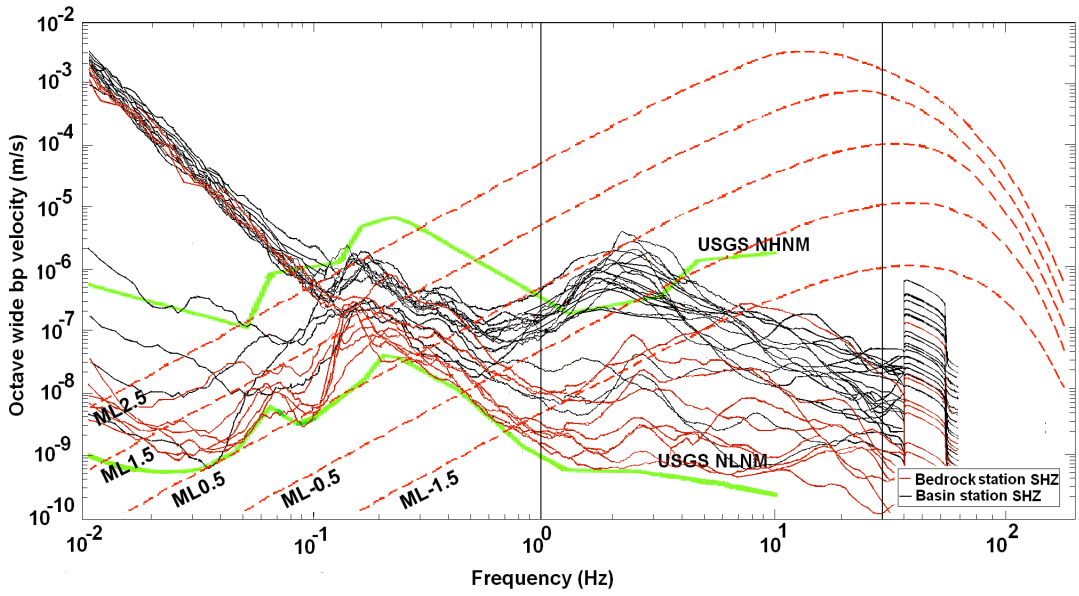

Figure 2: *Ambient seismic noise levels for the bedrock stations (red) and basin station (black) in comparison with theoretical Brune S-wave source spectra for local earthquakes with ML-1.5 to ML2.5. The US Geological Survey low and high noise model (Peterson, 1993) are*

indicated in green.The black vertical lines indicate the frequency band of interest for the earthquake location.

2.2. Earthquake data

Using a band-pass of 1-30 Hz, we visually screen the seismograms for local seismic events and manually pick the P-wave arrival times and the related picking uncertainties of the seismic events with SeisComP3 (Hanka et al. 2010). The onset of S-waves are too emergent to be reliably picked for the majority of events and are therefore not considered in this study. Within the analyzed 24 months, we detect 156 earthquakes within our network. The temporal distribution of the events is homogeneous over the observation period. The magnitudes of the events range from M_L0.5 to M_L1.9 (53 events between M_L0.5-1; 78 events between M_L1-1.5; 25 events >ML1.5). As explained in the previous section, earthquakes M_L<0.5 are not detectable by our network and we cannot confirm that we are not missing events below this threshold, particularly in the basin.

We are able to derive focal mechanisms for 9 events with P-wave first motion analysis and waveform matching (Table 1). The procedure is described in detail in section 3.2.

Table 1: Seismic events for which a focal mechanism could be determined

Date and time (yyymmdd)	**Lat (S)**	**Lon. (E)**	**Strike1/dip1/rake1**	**Strike2/dip2/rake2**	**Depth (Km)**	**Mag (ML)**	**Event Label**
2015/07/26 10:54:03.18	7.7315	112.5947	65/ 88/ -2	156 /87/ -178	9	1.5	6
2015/06/21 20:21:38.05	7.7378	112.5777	154/84 /162	246 /72/ 6	6	1.0	5
2015/05/04 10:42:47.82	7.5583	112.5744	327/ 69 /112	198/ 30/ 44	8	1.4	1
2015/03/01 10:56:21.42	7.5744	112.6435	337 /83/ -172	246 /82 /-6	12	0.9	2
2015/02/18 19:44:54.19	7.7383	112.5821	59 /50 /7	325/ 84 /140	4	1.0	4
2016/03/14 02:26:58.77	7.7203	112.6012	101/50/29	351/ 67 /136	9	1.3	7
2016/03/25	7.7475	112.5556	235/83/30	141 /60	12	1.7	3

04:40:06.93				/172			
2016/06/29 22:19:00.31	7.55	112.5933	234/82/29	140/58/170	13	1.2	8
2016/06/30 09:50:16.23	7.747	112.5885	237/85/32	143/62/174	9	1.4	9

2.2. Minimum 1D P-wave velocity model

We select a subset of 118 earthquakes that fulfil the following criteria: ≥8 P-phases, azimuthal gap ≤180°, root-mean-square (RMS) of initial location ≤0.5 s. The average picking uncertainty is estimated to be 0.12s. These events are used to calculate a so–called minimum 1D velocity model, which is subsequently used to relocate the entire earthquakes catalogue. The term minimum refers to the minimization of the average RMS misfit for all earthquakes by the inversion of travel-time data (Kissling et al. 1994). The model consists of a 1D average velocity structure of the region and station delays account for site-specific deviations from the 1D average. To simultaneously account for the hypocentral parameters, the 1D velocity structure and associated station delays, we use the inversion code VELEST (Kissling et al. 1995). As a reference site, we chose a broadband station with a low PSD-noise level, which is deployed on bedrock in the centre of the network and therefore has high-quality phase readings for most of the earthquakes (station BB08, blue triangle in Fig. 4). A regional 1D velocity model of Java (Koulakov et al. 2007), which is implemented in routine location procedures by the Indonesian Agency for Meteorology, Climatology and Geophysics (BMKG), was used as base for the initial model of the inversion (Fig. 3A, dashed line). As the inversion scheme does not account for layer thickness (Kissling et al. 1995), the optimal layering is determined through a trial-and-error process. To check the stability of our solution, we perform a series of inversions with different initial models. All results converge within a few iterations towards the final minimum P-wave velocity model (Fig. 3A, solid line). The final P-wave velocity model represents a relatively simple crustal structure with near-surface velocities of about 5.1 km/s and a gradual increase in velocity to 6.5 km/s in 11 km depth. The velocity below 11 km is almost constant, reaching 7 km/s at 30 km depth. Using the minimum 1D model, we could reduce the average RMS of single-event locations by approximately 10% with respect to the preliminary locations, using the Koulakov model (Fig. 3B, C).

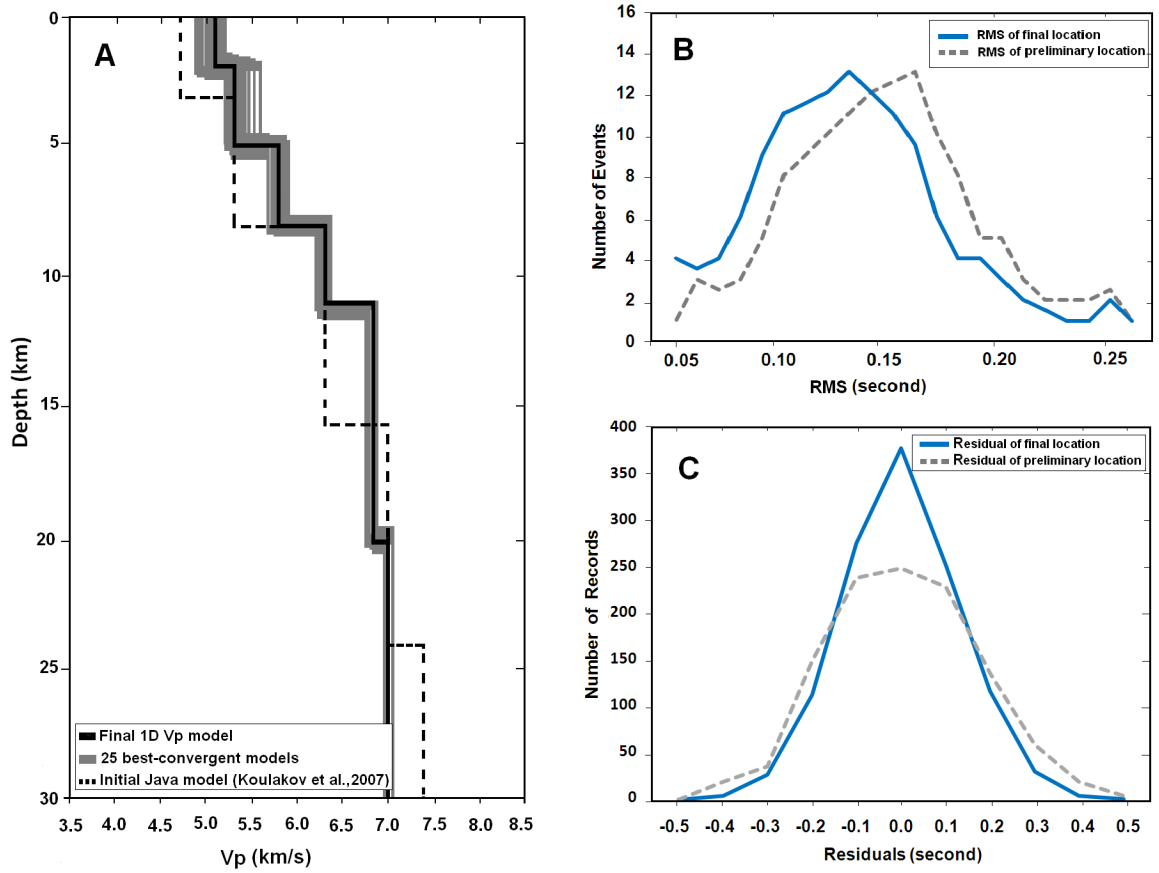

Figure 3: Minimum1D P-wave velocity model for the earthquake data set shown in Fig. 5. *A) Final minimum 1-D P-wave velocity model (thick black line), 25 best convergent models and the regional P-wave velocity model of Java (Koulakov et al. 2007). B) RMS values of 118 individual single-event locations, and C) travel-time residuals associated with the 118 events used in the inversion. Solid blue and dashed grey lines represent the final and preliminary location results, respectively.*

2.3. Station delays

Fig. 4 shows the calculated station delays associated with the minimum 1-D P-wave velocity model. Station corrections express deviations from the 1-D model due to 3-D structure with respect to a reference station (e.g. Kissling 1988). The correction of the reference station is defined as zero. Negative corrections (circles) indicate higher velocities compared to the reference station and positive corrections (crosses) indicate lower velocities. The station delays in Fig. 4 can be indicative for lateral variations of the near-surface geology (e.g., basement topography).

In this study, the station delays vary between -0.14s and +0.18s (Fig.4). Half of the sites have small station corrections with respect to the estimated picking uncertainty (<0.1s) and are

hence close to the noise of our data and are therefore not interpreted. The positive delay times in the surroundings of Lusi coincide with unconsolidated sediments dominating the near-surface geology of the basin (Abidin et al. 2009, Panzera et al. 2017, Mauri et al. 2017a, Mauri et al. 2017b). This is also in agreement with results of an ambient noise Rayleigh-wave tomography of the area that indicates strong negative shear-wave velocity anomalies around Lusi (Fallahi et al. submitted to JGR).

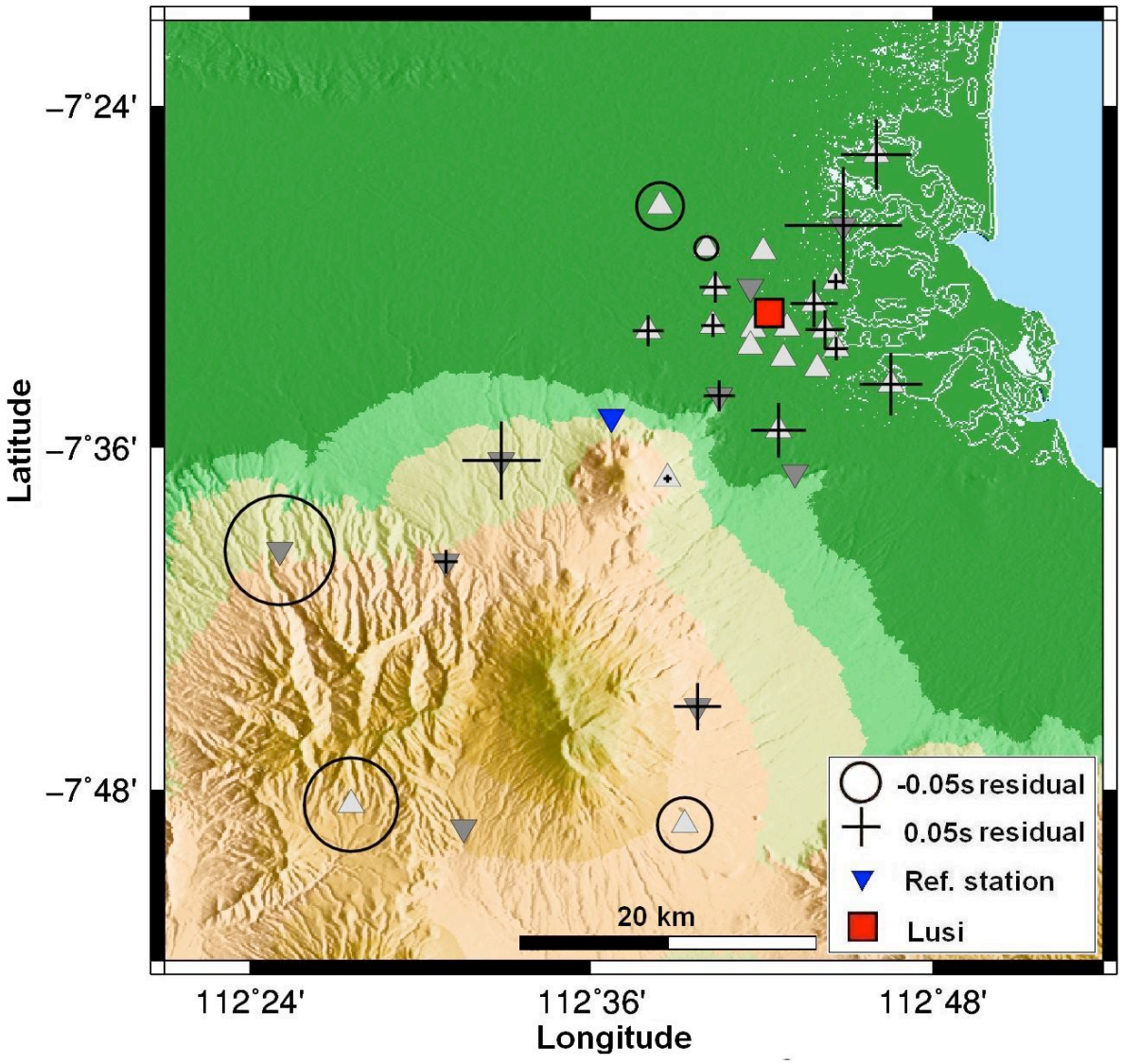

Figure 4: *Station delays as obtained from the VELEST inversion with respect to the reference site marked by the blue triangle. The station delays are only displayed for stations with more than five observations. Positive delays indicate velocities lower than the 1D average, or systematic delay of arrival time picks due to low SNR; negative station delays indicate a higher velocity compared to 1D average.*

3. Results

3.1. Earthquake relocalization

We use the minimum 1D P-wave velocity model to relocate all earthquakes in our catalog (Fig. 5). Formal horizontal location errors as derived by the VELEST location algorithm are on average 0.5 km and vertical errors are in the order of 2 km. About 95% of the observed events cluster around the Arjuno-Welirang volcanic complex. The majority of earthquakes occur in the upper crust between 8-13 km. We observe practically no seismicity in the area of Lusi (Fig. 5). As the comparison of the station noise levels with synthetic S-wave source spectra suggests (Fig.2), a theoretical detection threshold of M_L 0.5 might be achieved in this area. However, attenuation in the sedimentary basin is likely to affect the high-frequency part of the wave field and can therefore lead to significant deviations from the theoretical Brune-spectra for real data. We can therefore not entirely exclude the possibility that events $<M_L1.5$ are missed. Nevertheless, the observations of $M_L0.7$ events from the volcanic complex at stations in the sedimentary basin suggest that we should be able to detect such events in the basin.

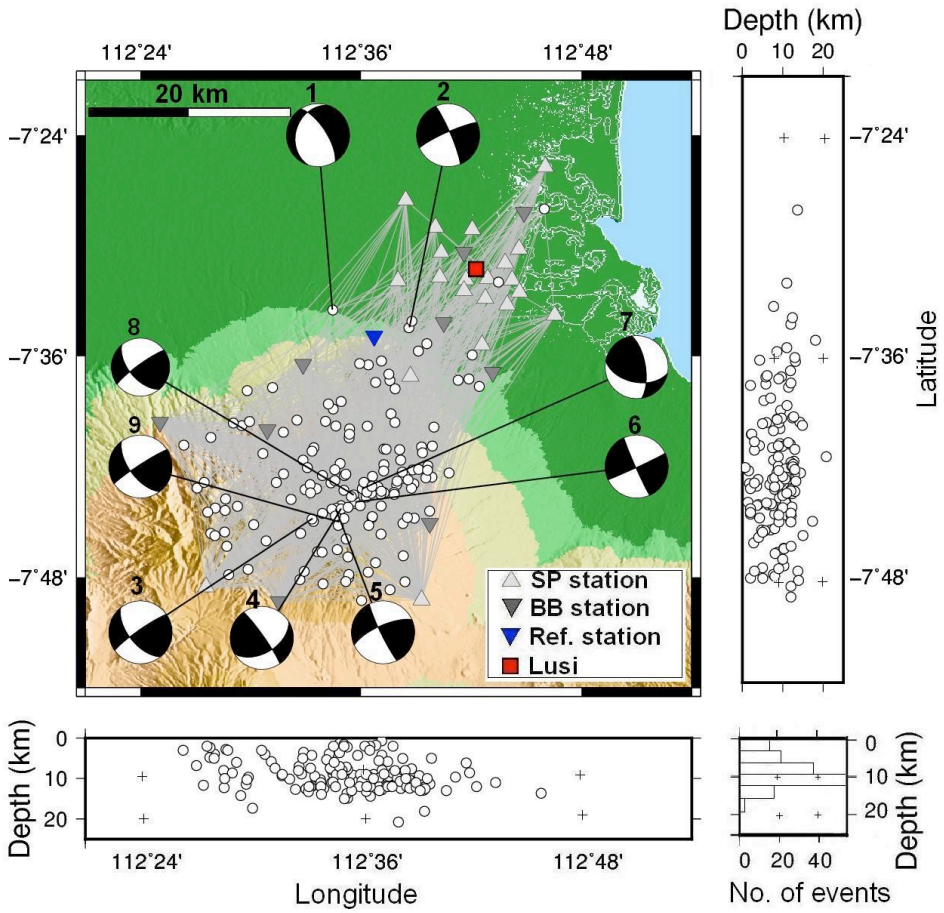

Figure 5: *Relocated micro-seismicity (M_L0.5-1.8) clustering around the Arjuno-Welirang volcanic complex. Fault plane solutions of larger events (Table 1) indicate a strike-slip deformation regime.*

3.2. Focal mechanism

For 9 events (Table 1) we obtain focal mechanisms through waveform matching using the ISOLA software (Sokos and Zahradnik, 2008, 2013). ISOLA calculates the moment tensor (MT) by matching P- and S-body waves with synthetics waveforms calculated in the minimum 1D crustal P-wave velocity model (Fig. 3A), using a least-squares algorithm. For the inversion, we use full waveforms (5-20Hz) from the 8 stations surrounding the earthquake that show the clearest records. Only solutions with a variance reduction greater than 65% are considered. Since waveform inversion can be ambiguous in the frequency range of such small magnitude events, the results are carefully cross-checked against P-wave first motions, which additionally constrain the obtained focal mechanisms (see supplementary material). Both

methods provide consistent results (see supplementary material) and we are therefore confident that our focal mechanism solutions are representative for the area.

The mechanisms of these 9 events indicate 7 predominantly strike-slip solutions, 1 thrust and 1 normal fault solution (Fig. 5). This is consistent with the general tectonic setting in this area (Istadi et al. 2012).

4. Discussion

The derived moment tensor solutions indicate a strike-slip component with fault planes striking NE-SW (sinistral) or NW-SE (dextral). Published literature (Lemigas, 1969, Situmorang et al., 1976, Moscariello et al., 2017) and field observations favor a sinistral movement. Situmorang et al., (1976) first pointed out that Java is divided by first order strike slip systems into three principal blocks developed in response to the large-scale tectonics. In particular, the southern shear system was interpreted to be linked to the NS lateral compression induced by the Northward movement of the Indian plate, relative to the Asian plate (Situmorang et al., 1976). In addition, Carn (2000) shows that a sinistral system, that extends towards the SW of Lusi and that links the Kawi-Butak and the Arjuno-Welirang volcanic complex. This possible link suggests that the arc is migrating from SW to the NE, with Kawi-Butak being the oldest and Pennagungan the youngest volcanic systems. Sawolo *et al.*, (2009), Mazzini et al. (2009), Istadi et al. (2009), and Moscariello et al 2017, proposed that the continuation of such NE-trending strike slip lineament is characterized by a widespread occurrence of diapiric structures piercing through the upper crust. In this context, Lusi would represent one of such piercement structures that reached the surface. Evidence of such diapiric growths as well as palaeo-venting systems is documented by 2D seismic data acquired in the north-eastern Javanese back-arc sedimentary basin (Istadi et al., 2009; Istadi et al., 2012). Field surveys at Lusi and surrounding areas also reveal sinistral shearing, like the sliken-side structures at the Watukosek escarpment as well as the numerous fractures that periodically appear (Fig. 6).

A

Figure 6: Surface-expression of the Watukosek Fault System at Lusi. A) View towards SW with the Arjuno Welirang complex in the background. Sinistral shearing is clearly visible. B) Examples of sliken-side structures along a NE-trending fault developed within Lusi's embankment.

Our analysis indicates that practically no significant seismic activity occurs beneath Lusi in the investigated 24 month period. Previous authors (Karyono *et al.*, 2016) showed the occurrence of tremors beneath Lusi that are related to its geysering activity. However, Karyono *et al.*, (2016) used a dense local array constituted of five seismic stations deployed within a $1km^2$ area around the Lusi craters . Our network is less dense, with only one station close to Lusi (i.e. in a distance of about 800 m from the main vents), which could explain why we miss these events. The apparent lack of detectable seismic activity in the East Java back-arc basin might be partly due to the particularly noisy site conditions that prevent detection of small events and the actual completeness might be higher than $M_L 0.5$. A possible alternative (or additional) explanation could be related to the significantly reduced shear wave velocities that characterize the part of the basin hosting Lusi (Fallahi et al. submitted to JGR). Negative shear-wave velocity anomalies (i.e. up to -15% from the average crustal velocities of the East Java Basin investigated by our network) could indicate the presence of fluids at depth that cause an elevated pore pressure, which may lead to a reduced friction along the potential fault zone. Under such conditions we would expect aseismic deformation or creep rather then stick-slip behavior, which is in agreement with ground-based GPS monitoring around the Lusi crater (Husein et al. 2016). The proposed aseismic deformation could also explain the previously observed tremor signals at Lusi (Karyono et al. 2016). The scattered distribution of seismicity in Figure 5 suggests that deformation is laterally distributed over a wider region rather than localized along a distinct fault zone.

The seismic network presented in this paper was also used to perform an ambient noise tomography (Fallahi et al. subm). However, towards the SW (i.e. beneath the volcanic arc) the network loses resolution and the study of Fallahi et al. was therefore not able to assess whether the AW volcanic complex sits upon the WFS. In any case, the AW volcanic system, PG volcano, Lusi, and other mud volcanoes in the region align along (and seem to develop upon) the direction of the WFS.

The seismic events occur rather deep inside the AW volcanic complex (8-13km). With our network, we did not observe swarms, propagation of seismicity nor tremor signals below the AW volcanic system. At this point, we cannot decide whether the seismic activity beneath the AW complex is connected to the activity of the WFS or linked to volcanic processes.

5. Conclusions

We observe a low rate of micro-seismic activity (M_L0.5-1.9; 156 events in 24 months) within our seismic network, which clusters below the Arjuno-Welirang volcanic complex in the upper crust (mainly 8-13 km). An analysis of the source mechanism of selected events indicates predominantly strike-slip faulting. In combination with surface geological observation, we interpret this regime to slip in sinistral direction. The surface deformations observed in the Lusi region are likely due to aseismic deformations rather than brittle rupture processes. These observations are consistent with the presence of fluid saturated sedimentary units present in the back-arc sedimentary basin.

Acknowledgements

The work was funded by the European Research Council under the European Union's Seventh Framework Programme Grant agreement n° 308126 (LUSI LAB project, PI A. Mazzini). We acknowledge the support from the Research Council of Norway through its Centers of Excellence funding scheme, Project Number 223272. A. Obermann received funds from the European Community's Seventh Framework Programme Grant agreement n°608553 (Project IMAGE). We thank the Geophysical Instrument Pool Potsdam (GIPP) for providing the instruments for the SEED experiment in the framework of the LUSI LAB project. Anne Obermann and Matteo Lupi are part of the SCCER collaborative environment. Matteo Lupi acknowledges SNF (projects PYAPP2_166900 and PZ00P2_154815)**.** We thank Prof. Edi Kissling for constructive discussions. We wish to thank Florian Fuchs, Sebastiano d'Amico and an unknown reviewer for their constructive comments.

References

Abidin, H.Z., Davies, R.J., Kusuma, M.A., Andreas, H. and Deguchi, T., 2009. Subsidence and uplift of Sidoarjo (East Java) due to the eruption of the Lusi mud volcano (2006–present). *Environmental geology*, *57*(4), pp.833-844.

Bormann, P. (1998), Conversion and comparability of data presentations on seismic background noise, J. Seismolog., 2, 37–45.

Brune, J. N. (1970), Tectonic stress and the spectra of seismic shear waves from earthquakes, J. Geophys. Res., 75, 4997–5009.

Brune, J. N. (1971), Correction, J. Geophys. Res., 76, 5002.

Carn, S.A., 2000. The Lamongan volcanic field, East Java, Indonesia: physical volcanology, historic activity and hazards. *Journal of Volcanology and Geothermal Research*, *95*(1), pp.81-108.

Clinton, J. F., and T. H. Heaton (2002), Potential advantages of a strong-motion velocitymeter over a strong-motion accelerometer, Seismol.Res. Lett., 73, 332–342.

Collignon, M., Schmid, D. W., and A., M., 2016, Fluid flow modeling at the Lusi mud eruption, East java, Indonesia. : Geophysical Research Abstracts, EGU General Assembly 2016, v. Vol. 18, EGU2016-7149-1.

Cyranoski, D., 2007, Indonesian eruption: muddy waters: Nature v. 445, p. 812-815.

Fallahi, M., Obermann, A., Lupi, M., Karyono, K., Mazzini, A. The Lusi eruption plumbing system revealed by ambient noise tomography, submitted to JGR

Hanka, W., Saul, J., Weber, B., Becker, J., Harjadi, P., Fauzi; GITEWS Seismology Group (2010). Real-time earthquake monitoring for tsunami warning in the Indian Ocean and beyond. Natural Hazards and Earth System Sciences, 10, 2611–2622, doi:10.5194/nhess-10-2611-2010.

Husein, A., Mazzini, A., Hadi, S., Santosa, B., Charis, M., & Irawan, D. (2016, April). Ground-based GPS monitoring at the Lusi eruption site and external perturbations. In *EGU General Assembly Conference Abstracts* (Vol. 18, p. 368).

Inguaggiato, S., Mazzini, A., Vita, F., and Sciarra, A., 2017, The Arjuno-Welirang Volcanic Complex and the connected Lusi system: geochemical evidences: Marine & Petroleum Geology, v. (this volume).

Istadi, B. P., Pramono, G. H., Sumintadireja, P., and Alam, S., 2009, Modeling study of growth and potential geohazard for LUSI mud volcano: East Java, Indonesia: Marine and Petroleum Geology, v. 26, p. 1724-1739.

Istadi, B., Wibowo, H. T., Sunardi, E., Hadi, S., and Sawolo, N., 2012, Mud Volcano and Its Evolution: In tech, v. ISBN 978-953-307-861-8, p. 375-434.

Karyono, K., Obermann, A., Lupi, M., Masturyono, M., Hadi, S., Syafri, I., Abdurrokhim, A., and Mazzini, A., 2017, Lusi, a clastic dominated geysering system in Indonesia recently explored by surface and subsurface observations: Terra Nova, 29(1), 13-19 p. doi: 10.1111/ter.12239.

Kissling, E. (1988). Geotomography with local earthquake data. Reviews of Geophysics, 26(4), 659-698.

Kissling, E., Ellsworth, W.L., Eberhart-Phillips, D. and Kradolfer, U., 1994. Initial reference models in local earthquake tomography. *Journal of Geophysical Research: Solid Earth*, *99*(B10), pp.19635-19646.

Kissling, E., Kradolfer, U. and Maurer, H., 1995. Program VELEST user's guide-Short Introduction. *Institute of Geophysics, ETH Zurich*.

Koulakov, I., Bohm, M., Asch, G., Lühr, B.G., Manzanares, A., Brotopuspito, K.S., Fauzi, P., Purbawinata, M.A., Puspito, N.T., Ratdomopurbo, A. and Kopp, H., 2007. P and S velocity structure of the crust and the upper mantle beneath central Java from local tomography inversion. *Journal of Geophysical Research: Solid Earth*, *112*(B8).

LEMIGAS/BEICIP, 1969, North-East Java Basin, unpublished report, Lemigas, Jakarta

Lupi, M., Saenger, E.H., Fuchs, F. and Miller, S.A., 2013. Lusi mud eruption triggered by geometric focusing of seismic waves. *Nature Geoscience*, *6*(8), pp.642-646.

Lupi, M., Saenger, E.H., Fuchs, F. and Miller, S.A., 2014. Corrigendum: Lusi mud eruption triggered by geometric focusing of seismic waves. *Nature Geoscience*, *7*(9), pp.687-688.

Mauri, G., Husein, A., Mazzini, A., Karyono, K., Obermann, A., Bertrand, G., and Miller, S. A. (2017a). Constraints on density changes in the funnel-shaped caldera inferred from gravity monitoring of the Lusi mud eruption. *Marine and Petroleum Geology*.

Mauri, G., Husein, A., Mazzini, A., Irawan, D., Sohrabi, R., Hadi, S., and Miller, S. A. (2017b). Insights on the structure of Lusi mud edifice from land gravity data. *Marine and Petroleum Geology*.

Mazzini, A., Svensen, H., Akhmanov, G. G., Aloisi, G., Planke, S., Malthe-Sorenssen, A., and Istadi, B., 2007, Triggering and dynamic evolution of the LUSI mud volcano, Indonesia: Earth and Planetary Science Letters, v. 261, p. 375-388.

Mazzini, A., Nermoen, A., Krotkiewski, M., Podladchikov, Y., Planke, S., and Svensen, H., 2009, Strike-slip faulting as a trigger mechanism for overpressure release through piercement structures. Implications for the Lusi mud volcano, Indonesia: Marine and Petroleum Geology, v. 26, p. 1751-1765.

Mazzini, A., Etiope, G., and Svensen, H., 2012, A new hydrothermal scenario for the 2006 Lusi eruption, Indonesia. Insights from gas geochemistry: Earth and Planetary Science Letters, v. 317, p. 305-318.

Mazzini, A., Scholz, F., Svensen, C., Hensen, C., and Hadi, S., 2017, The geochemistry and origin of the hydrothermal water erupted at Lusi, Indonesia: Marine & Petroleum Geology, v. https://doi.org/10.1016/j.marpetgeo.2017.06.018.

Moscariello, A., Do Couto, D., Mondino, F., Booth, J., Lupi, M., and Mazzini, A., this issue, Genesis and evolution of the Watukosek fault system in the Lusi area (East Java): (this issue) Marine & Petroleum Geology.

McNamara, D. E., and R. Boaz (2006), Seismic noise analysis system using power spectral density probability density functions:A stand-alone software package, U.S. Geol. Surv. Open File Rep., NO. 2005-1438, U.S. Geol. Surv., Reston, Va.

Sawolo, N., Sutriono, E., Istadi, B.P. and Darmoyo, A.B., 2009. The LUSI mud volcano triggering controversy: Was it caused by drilling?. Marine and Petroleum Geology, 26(9), pp.1766-1784.

Situmorang, B., Siswoyo, E.T., Paltrinieri, F., 1976, Wrench fault tectonicts and aspects of hydrocarbon accumulation in Java, 5th Annual Convention Proceedings, Volume 2, pages 53-67.

Panzera F., D'Amico, S., Lupi, M., Mauri, G., Karyono, K., & Mazzini, A. (2017). Lusi hydrothermal structure inferred through ambient vibration measurements. *Marine and Petroleum Geology*.

Peterson, J. (1993), Observations and modeling of seismic background noise, U.S. Geol. Surv. Tech. Rep. 93-322, US Geol. Surv., Albuquerque,N. M.

Sciarra, A., Mazzini, A., Inguaggiato, S., Vita, F., Lupi, A., and Hadi, S., 2017, Radon and carbon gas anomalies along the Watukosek fault system and Lusi mud eruption, Indonesia: (this issue) Marine & Petroleum Geology.

Sokos, E.N. and Zahradnik, J., 2008. ISOLA a Fortran code and a Matlab GUI to perform multiple-point source inversion of seismic data. *Computers & Geosciences*, *34*(8), pp.967-977.

Sokos, E. and Zahradník, J., 2013. Evaluating centroid-moment-tensor uncertainty in the new version of ISOLA software. *Seismological Research Letters*, *84*(4), pp.656-665.

Vanderkluysen, L., Burton, M. R., Clarke, A. B., Hartnett, H. E., & Smekens, J. F., 2014. Composition and flux of explosive gas release at LUSI mud volcano (East Java, Indonesia). *Geochemistry, Geophysics, Geosystems*, *15*(7), 2932-2946.

Van Noorden, R., 2006, Mud volcano floods Java: Nature, v. doi:10.1038/news060828-1